INTERNAL REPORT #72

BACKGROUND FLUXES OF H AND He ISOTOPES PRODUCED IN THE WINDOWS OF COSMIC RAY TELESCOPES

by

H. Breneman

R. A. Mewaldt

Space Radiation Laboratory

California Institute of Technology

Pasadena, California

7-5-79

I INTRODUCTION

Cosmic ray telescopes of recent design frequently include small amounts of inactive material within the viewing cone defined by the active detectors of the telescope. As an example, consider the "window" in a hypothetical design shown in Figure 1. The flux of high energy galactic cosmic rays produces an essentially constant rate of nuclear interactions with nuclei of the window. If the window is not surrounded by active anticoincidence shielding, a fraction of the low energy evaporation products of these interactions will be detected by the telescope, thereby masquerading as low energy cosmic rays. This "background" is most important for relatively rare cosmic ray species such as ^{2}H, ^{3}He and the elements Li, Be, and B. This report makes quantitative estimates of this background mechanism for the isotopes of hydrogen and helium, for which reasonable cross section values are available. The results are applied to several SRL telescopes of recent vintage, and compared with flight data where possible.

II THE SPECTRA OF SECONDARY EVAPORATION PRODUCTS

N_i (E_p), the evaporation yield of species i per inelastic event, was determined for values of the incident proton energy E_p of 500, 1000, 1500, 2000, 2500 and 3000 MeV for each of the five species ^1H, ^2H, ^3H, ^3He and ^4He. This data was obtained from the MECC-7 Intranuclear Cascade Calculation produced at ORNL by Bertini (1963) for protons of energy E_p on ^{27}Al. The data, available on microfiche in SRL library, appears on Frame 1 of the Evaporation Code. Neutron data were irrelevant since only charged particles could be detected. For other values of E_p, N_i was assumed to be a piecewise linear function of log E_p. When plotted against log E_p, N_i between two successive given values of E_p was obtained by linear interpolation; below E_p = 500 MeV it was taken to approach zero linearly at a rate such that N_i = 0 at E_p = 50 MeV (unless extrapolation of the 500 - 1000 MeV segment below 500 MeV would result in N_i = 0 at a value of E_p less than 50 MeV, in which case that extrapolation was used for N_i), and above E = 3000 MeV, N_i was taken as constant at its value at 3000 MeV. $N_i(E_p)$ values for the five species of interest are summarized in Figure 2.

The evaporation spectrum of product species i was assumed to have the form

$$\frac{dN_i}{dT_i} = A_i(E_p)\ e^{-B_i(E_p)T_i} \quad \text{particles/(MeV/nucleon)} \qquad (1)$$

where T_i = kinetic energy/nucleon of species i. The coefficients $A_i(E_p)$, $B_i(E_p)$ were obtained for E_p = 500, 1000, 1500, 2000, 2500, 3000 MeV from evaporation spectra for the five species H^1, H^2, H^3, He^3 and He^4 (Bertini, 1963). Each of these spectra was fit to the form (1) using FORTRAN program GRIDFIT, with A_i and B_i treated as adjustable parameters. Once the best fit was obtained, the values of A_i were renormalized by the condition

$$\int_0^\infty \frac{dN_i}{dT_i}(E_p)\ dT_i = N_i(E_p) = \frac{A_i(E_p)}{B_i(E_p)} \qquad (2)$$

for each of the six values of E_p, where $B_i(E_p)$ is the best-fit value and $N_i(E_p)$ had the value obtained above. This procedure provided A_i and B_i at E_p = 500, 1000, 1500, 2000, 2500 and 3000 MeV. For general values of E_p, $B_i(E_p)$ was taken to be a linear function of log E_p, determined as a best fit of the given points (Figure 3). With values of B_i and N_i known for all E_p, $A_i(E_p)$ is then determined for any E_p by the normalization condition (2). The renormalized A_i's differed slightly from those initially obtained by fitting the Bertini evaporation spectrum data since these spectra had an upper-limit cutoff of 25 MeV for ^1H and 50 MeV for ^2H, ^3H, ^3He, and ^4He, while the renormalization involved integration over all values of E_p from 0 to ∞. In using the GRIDFIT program for curve fitting, the points to be fit were plotted and first-guess values of the parameters, required by the program, were obtained by inspection of the plot. Accuracy of the parameters finally obtained depended on the quality of the statistics in the Bertini spectra, which was much better, for instance, for ^2H and ^4He than for ^3H and ^3He, as is evident in Figure 3.

Curves for dM_i/dT_i (number of particles of species i per MeV/nucleon per interaction) were obtained by numerically evaluating

$$\frac{dM_i}{dT_i} = \int_0^{E_{max}} \frac{dJ_p}{dE_p} \frac{dN_i}{dT_i} (E_p)\, dE_p \Bigg/ \int_0^{E_{max}} \frac{dJ_p}{dE_p}\, dE_p \qquad (3)$$

for each species at several values of T_i. FORTRAN program INTEGR8 was written, incorporating library program SIMSON for numerical integration. In principle, the integrals should have an upper limit of ∞, but the integration was cut off at the value E_{max} such that

$$\int_0^{E_{max}} \frac{dJ_p}{dE_p} \, dE_p = 0.99 \int_0^{\infty} \frac{dJ_p}{dE_p} \, dE_p \tag{4}$$

For convenience, the incident cosmic ray proton spectrum was assumed to be of the form

$$\frac{dJ_p}{dE_p} = \frac{K}{(E_p + E_o)^{\gamma}} \text{ protons /m}^2 \text{ sr sec MeV} \tag{5}$$

where E_p is the proton energy and K, E_o and γ are empirical constants. Solar minimum proton data as summarized by Webber and Lezniak (1973) gave dJ_p/dE_p as a function of E_p for E_p up to 50,000 MeV. This data was fit to the form (5) with K, E_p and γ as adjustable parameters using program GRIDFIT. The lowest E_p value used in the fitting was also varied, since it was known that the data did not agree with the assumed form for $E_p \leqslant 500$ MeV. After fitting the data with the lowest value of E_p at 341, 500, and 734 MeV, it was decided that 734 MeV gave the best fit. The resulting optimum values of the parameters were

$$K = 3.32 \times 10^9, \; E_o = 1734 \text{ MeV}, \; \gamma = 2.75 \qquad (6)$$

The integrals in Eq. (4) could now be evaluated analytically:

$$\int \frac{dJ_p}{dE_p} \, dE_p = \int \frac{K}{(E_p + E_o)^\gamma} \, dE_p = \frac{-K}{(\gamma-1)\,(E_p + E_o)^{\gamma-1}}$$

$$J_p = \int_0^\infty \frac{dJ_p}{dE_p} \, dE_p = \frac{K}{(\gamma-1)\, E_o^{\;\gamma-1}}$$

With K, E_o, and γ as given by (6), this yields

$$J_p = \int_0^\infty \frac{dJ_p}{dE_p} \, dE_p = 4061/\text{m}^2 \text{ sec sr}, \; E_{max} = E_o(100^{\frac{1}{\gamma-1}} - 1) = 22346 \text{ MeV}$$

dM_i/dT_i was evaluated for each particle at values of T_i between 0 and 50 Mev/nucleon. (see Figure 4).

Program INTEGR8 was modified to calculate M_i = total number of species i produced per interaction, averaged over energy:

$$M_i = \int_0^{E_{max}} \frac{dJ_p}{dE_p} N_i(E_p)dE_p \Bigg/ \int_0^{E_{max}} \frac{dJ_p}{dE_p} dE_p$$

where E_{max}, same value as before, replaced ∞ as upper limit of integration. The values obtained for M_i appear in Table I.

The number of interactions per second Q_p occurring in a telescope window due to incident protons is given by

$$Q_p = 4\pi J_p \frac{(xA_w)\,\sigma}{A\,m_p}$$

where A_w is the area of the window within the telescope's view, x the window thickness in g/cm^2 (equal to the geometric thickness multiplied by the density ρ), A the mass number of the window material, m_p the proton mass and σ the total interaction cross section for protons on the window material.

σ in mb is given approximately by

$$\sigma = 50\ A^{2/3}\ \text{mb}$$

To take into account the interactions of incident particles with $Z \geq 2$, Q_p is multiplied by an additional factor C given by

$$C = \frac{\sum N(Z')\ \ \sigma\ (A')}{N(1)\ \ \ \sigma\ (1)}$$

where

$\sigma\ (A') = \pi\ (R + r')^2$ mb, $R = r_o\ A^{1/3}$, $r' = r_o(A')^{1/3}$

$r_o = 1{\cdot}17 \times 10^{-13}$ cm

for $A' \neq 1$,

$$\sigma\ (1) = \pi\ (R_o\ A^{1/3})^2\ \text{mb},\quad R_o = 1.2 \times 10^{-13}\ \text{cm}$$

and N(Z') is the relative cosmic ray abundance of element Z'. The sum is over all elements Z' with A' taken to be the weighted average mass number for element Z'. Summing up through Z' = 27 and using cosmic ray abundances given by Lezniak and Webber (1978) for energies greater than 450 MeV/nucleon, C was found to have the value

$$C = 1.25$$

from which the total number of interactions per second in the telescope window is given by

$$Q = 1.25\ Q_p = 1.25\ \frac{4\pi\ J_p\ \sigma\ x\ A_w}{Am_p}$$

The evaporation species produced in the window are assumed to be distributed isotropically, so the fraction detected by the telescope is given by

$$f = \frac{G}{4\pi\ A_w}$$

where G is the geometry factor for the window telescope combination.

The flux of evaporated particles detected is given by

$$\frac{dJ_i}{dT_i}(T_i) = 1.25\ J_p\ \frac{\sigma x}{Am_p}\ \frac{dM_i}{dT_i}\ (T_i) \qquad (5)$$

III EXAMPLES OF WINDOW-PRODUCED BACKGROUND

Equation (5), together with the results obtained above for dJ_i/dT_i and J_p, allow the calculation of the background flux due to evaporation for specific telescope designs; these results appear in Table II. The window thicknesses used are for actual SRL detector systems. In some cases the windows were made of aluminized Mylar instead of aluminum foil. Here it was assumed that interactions with C or O nuclei are equivalent to those with Al nuclei, so that the results obtained in Section II for dM_i/dT_i (Figure 4) are still valid. It then follows that 1 mg/cm^2 of Mylar ($C_{12}H_{14}O_4$, $\rho = 1.26\ g/cm^3$) is equivalent to 1.276 mg/cm^2 of Al.

Table II also includes an additional contribution due to high energy neutron interactions (see Section IV). The proton (actually charged nuclei) contributions are defined to be = 1, and the estimated neutron contributions are shown as a fraction of this.

For an explanation of the Voyager HET entry see Section V.

IV. HIGH ENERGY NEUTRON INTERACTIONS

An additional source of interactions in telescope windows is due to high energy cascade neutrons produced in surrounding material of the spacecraft by the interactions of high energy cosmic rays. These neutrons have energies up to and including the incident cosmic ray energy/nucleon. Active collimation will have little effect on this contribution. A rough estimate of its significance follows.

For a spacecraft of mass M, assumed to consist of aluminum, the number of high energy cascade neutrons produced per second is

$$Q_n \simeq 1.25\ (4\pi)\ J_p \frac{\sigma}{27\ M_p}\ MN_n$$

where J_p is the integral proton flux, $\sigma \simeq 450$ mb is the interaction cross section for protons on aluminum, and N_n is the average neutron multiplicity. From Bertini (1963) we find $N_n \simeq 3$ at 2.0 GeV. Assuming spherical symmetry, with the telescope located γ cm from the S/C center of mass, the secondary neutron flux at the window $(cm^2\text{-sr-sec})^{-1}$ is:

$$J_n \simeq \frac{Q_n}{4\pi Y^2} \left(\frac{1}{2\pi}\right),$$

and the ratio of the neutron to proton flux is

$$\frac{J_n}{J_p} \simeq \frac{1.25}{2\pi Y^2} \frac{\sigma}{27M_p}\ MN_n$$

For ISEE-3:

$$Y \simeq 80 \text{ cm}$$

$$M_n \simeq 4 \times 10^5 \text{g}$$

and we find $J_n/J_p \simeq 0.4$, which constitutes the neutron contribution in Table II. For IMP-7 and 8, similar in size to ISEE-3, the situation is more complicated due to anticoincidence shielding in these telescopes (see Internal Report No. 68).

The EIS on IMP-8 has two windows: one of 0.8 g/cm^2 Mylar (unshielded) and one of 2.4 g/cm^2 (shielded, therefore no proton contribution). Therefore the total neutron contribution is 0.4 + 3(0.4) = 1.6 times proton contribution. For IMP-7 the only contribution is from neutrons in the 2.4 mg/cm^2 window (shielded). Voyager is a much more massive S/C, but less dense and unsuited for the spherical symmetry assumption. We therefore naively use the same 0.4 factor as above. These neutron estimates are included in Table II.

V. COMPARISON WITH FLIGHT DATA

Figure 5 compares the calculated background (Table II and Figure 4) for IMP-8 with ^{2}H and ^{3}He measurements from IMP-7 and IMP-8 (1973-1974). Note that the ^{2}H background exceeds the fit spectrum below $\simeq$ 6 MeV/nucleon. A slightly greater background problem is expected in HIST.

Voyager HET data presents a possible chance to measure this background. If we consider B1 in HET as a window (2 mm of silicon) then B1·B2·ΣC events include background from interactions in B1. Figure 6 shows the measured "fluxes" of ^{1}H, ^{2}H, and ^{3}H determined from B2 and ΣC pulse-heights, but using the B1·B2·ΣC geometry factor. Similarly Figure 7 shows ^{3}He and ^{4}He data. The "fluxes" far exceed the expected quiet-tone levels for galactic particles, and the ^{3}H data especially is compelling evidence that these particles are background. In general, these events had random B1 pulse-heights, consistent with the background mode described in this report. Note that the measurements exceed the ^{2}H and ^{3}H calculations by $\geq$ X 5, although the relative proportions of the isotopes and the spectral shapes are in general agreement with the calculated yields. The ^{3}He and ^{4}He background far exceeds the calculations and may require a different explanation.

The following consideration will lead to additional background satisfying the HET event selection criteria. In addition to B1, there is a large amount of inactive material within the viewing cone of B2·ΣC, which can serve as an additional site for interactions. Some of these interacting nuclei will also trigger B1, either themselves, or by means of their interaction products, knock-on electrons, etc. Thus the "effective thickness" of B1 for interactions may be much greater than 2 mm of silicon. Fortunately, the B1 pulse height for these events is, in general, not consistent with B2 and ΣC, so these events can be to a large extent eliminated.

A second type of background, not considered in this report, may come from incident heavy nuclei that fragment in the window. For example: $^{12}C + ^{27}Al \longrightarrow ^{3}He + ^{9}Be + ^{27}Al$. For this type of background to be important would require that the energetic ^{3}He and ^{9}Be separate such that only one of these hits any of the detectors, including guards. The separation angle of fragments is generally only a degree or so except at low energies ($\leqslant$ 100 MeV/nuc).

REFERENCES:

Bertini, H. W., Oak Ridge National Laboratory Reports #3383 (1962) and #3433 (1963)

Lezniak, J. A., and W. R. Webber, Astrophys. J. 223, 676-696 (1978)

Webber, W. R., and J. A. Lezniak, Astrophys. Sp. Sci. 30, 361 (1974)

TABLE I

EVAPORATION YIELD PER INTERACTION, AVERAGED OVER ENERGY, FOR THE SPECIES ^1H, ^2H, ^3H, ^3He, ^4He

Species	M_i (number per interaction)
^1H	1.2930
^2H	0.2361
^3H	0.0395
^3He	0.0574
^4He	0.4308

TABLE II

BACKGROUND FLUX LEVELS FOR VARIOUS COSMIC RAY TELESCOPES

Spacecraft	Telescope	Window Al	Window Mylar	Window Total Al Eqv.	Anti Shield	Relative Contrib. P	Relative Contrib. N	Total Scale Factor for Figure 4
ISEE-3	HIST	1.62	0.80	2.64	No	1	0.4	1.9×10^{-5}
IMP-7	EIS	0.0	2.40	3.06	Yes	0	0.4	3.3×10^{-6}
IMP-8	EIS	0.0 0.0	0.8 2.4	1.02 3.06	No Yes	1 0	0.4 0.4	1.4×10^{-5}
Voyager	LET	0.81	0.0	0.81	No	1	0.4	6.0×10^{-6}
Voyager	HET	466 (B1)		466	No	1	0.4 ?	3.4×10^{-3}

FIGURE CAPTIONS

Fig. 1 Geometry of evaporation background events for a typical telescope design.

Fig. 2 Evaporation yield per inelastic event for the species ^{1}H, ^{2}H, ^{3}H, ^{3}He and ^{4}He, for protons of energy E_p incident on ^{27}Al. Values for E_p in the 500-3000 MeV range are based on data by Bertini (1963) and were extrapolated to other energies. Note that proton line is scaled down by a factor of 3.

Fig. 3 Coefficient B_i in Eq. (1) for the evaporation spectrum of the species ^{1}H, ^{2}H, ^{3}H, ^{3}He and ^{4}He as a function of incident proton energy E_p. Lines are obtained as a best fit to data by Bertini (1963) for E_p in the range 500-3000 MeV.

Fig. 4 Number of particles per MeV/nucleon per interaction for the evaporation product species ^{1}H, ^{2}H, ^{3}H, ^{3}He and ^{4}He as a function of their kinetic energy per nucleon T_i. Curves were obtained by numerical integration of Eq. (3).

Fig. 5 Comparison of the calculated background for IMP-8 with measured quiet time fluxes and upper limits.

Fig. 6 Comparison of the calculated H isotope background for Voyager HET B1·B2·ΣC events with measured background fluxes.

Fig. 7 Same as Figure 6, but for He isotopes.

FIG. 1

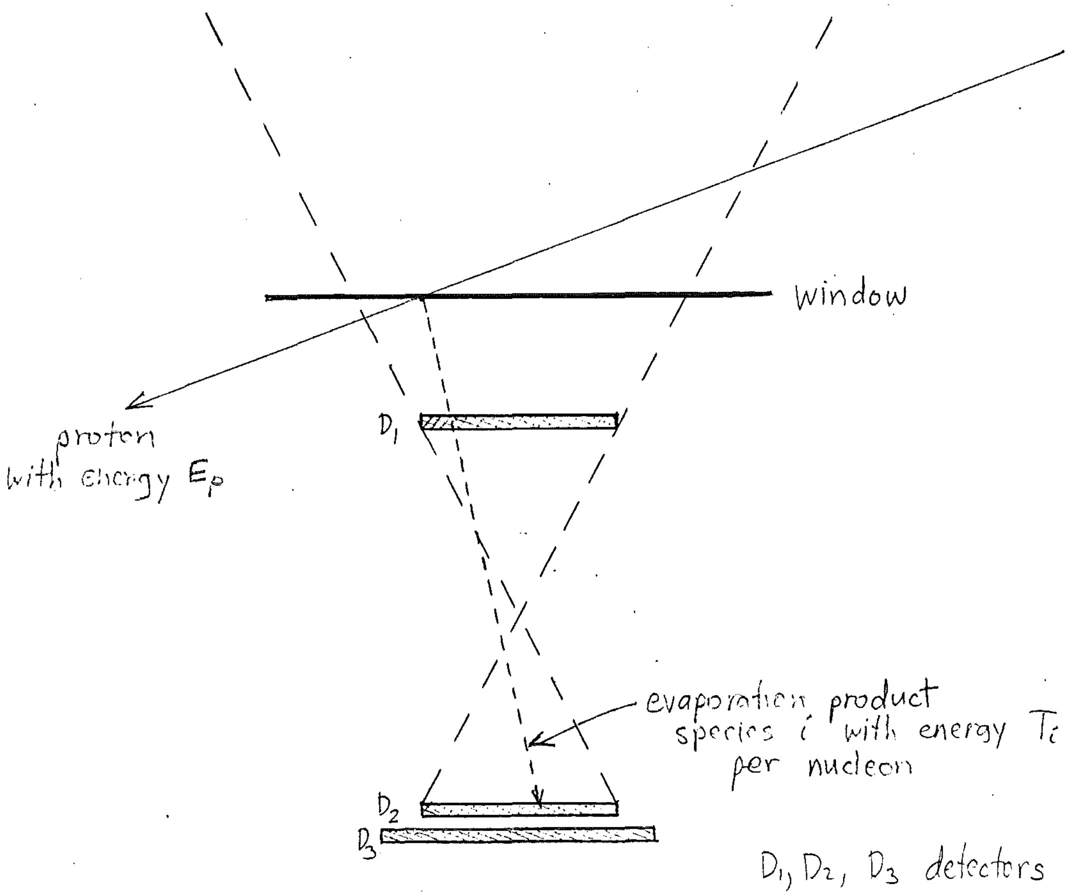
window
proton
with energy E_p
D_1
evaporation product
species i with energy T_i
per nucleon
D_2
D_3
D_1, D_2, D_3 detectors

K+E SEMI-LOGARITHMIC • 3 CYCLES X 70 DIVISIONS
KEUFFEL & ESSER CO. MADE IN U.S.A.

FIG. 2

46 5490

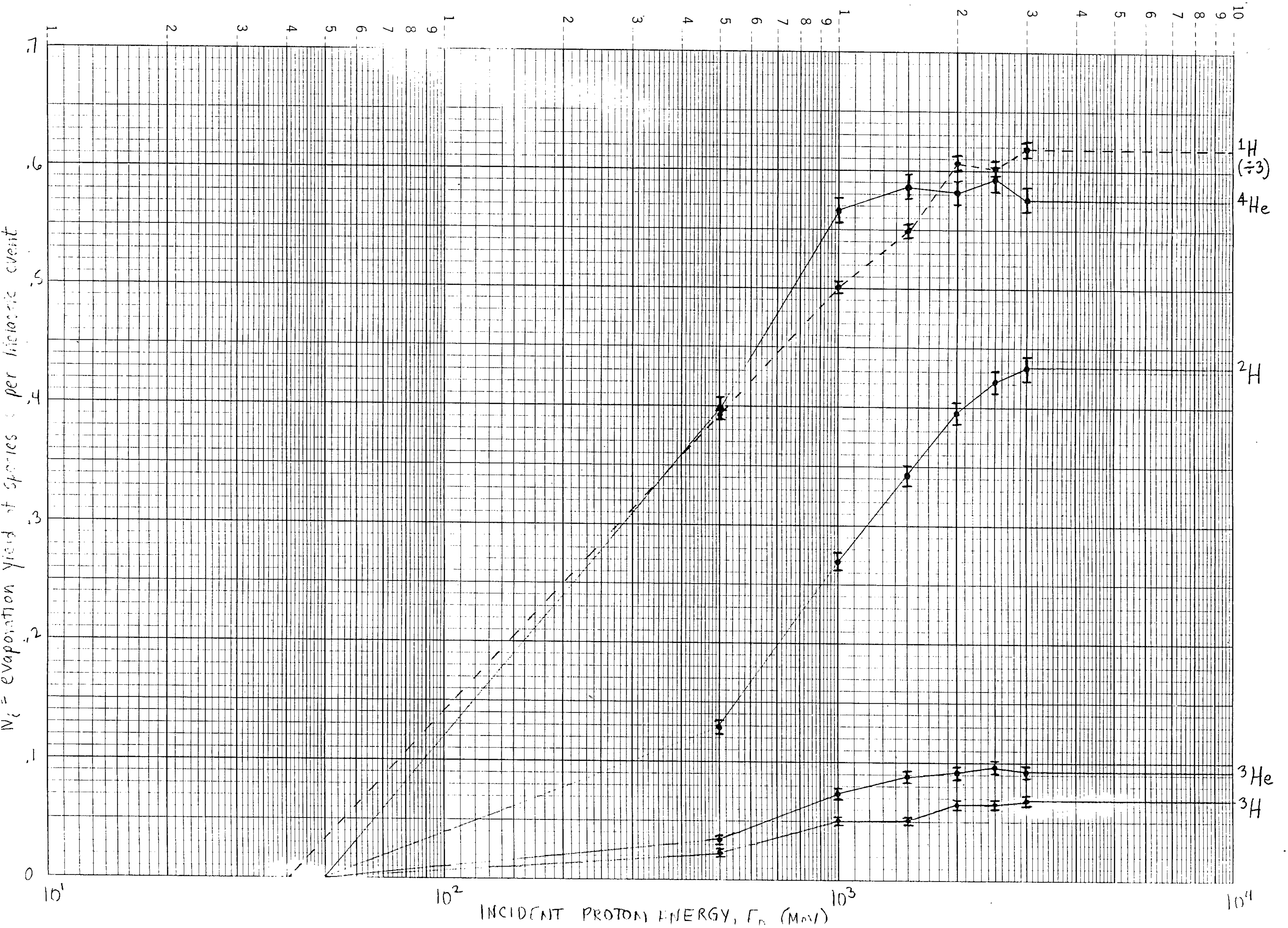

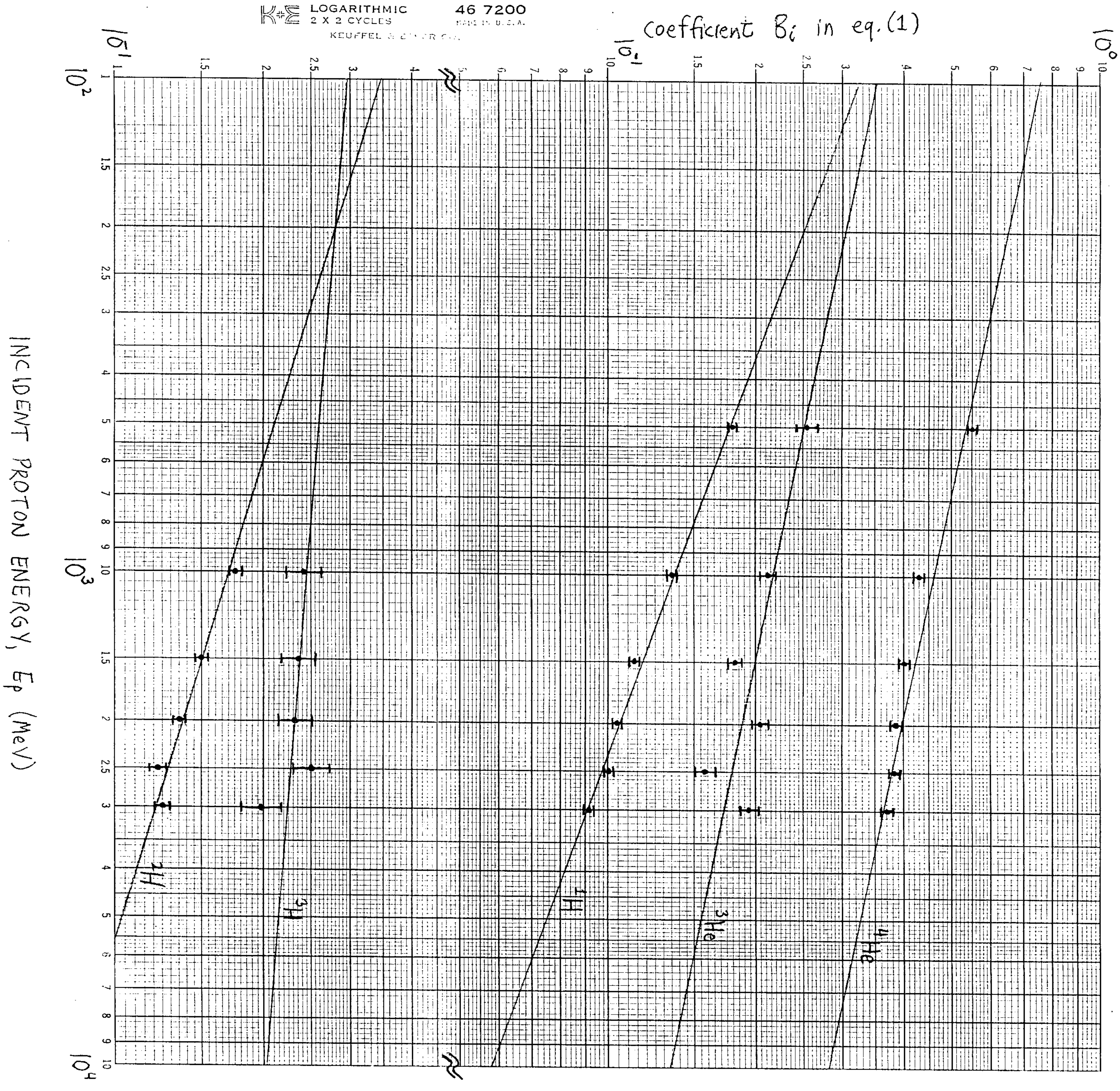

K+E LOGARITHMIC 2 X 2 CYCLES 46 7200
KEUFFEL & ESSER CO.
coefficient B_i in eq.(1)
10^{-1}
10^{-1}
10^{0}
10^{2}
10^{3}
10^{4}
INCIDENT PROTON ENERGY, E_p (MeV)
^2H
^3H
^1H
^3He
^4He

FIG. 3

FIG. 4

EVAPORATION YIELDS

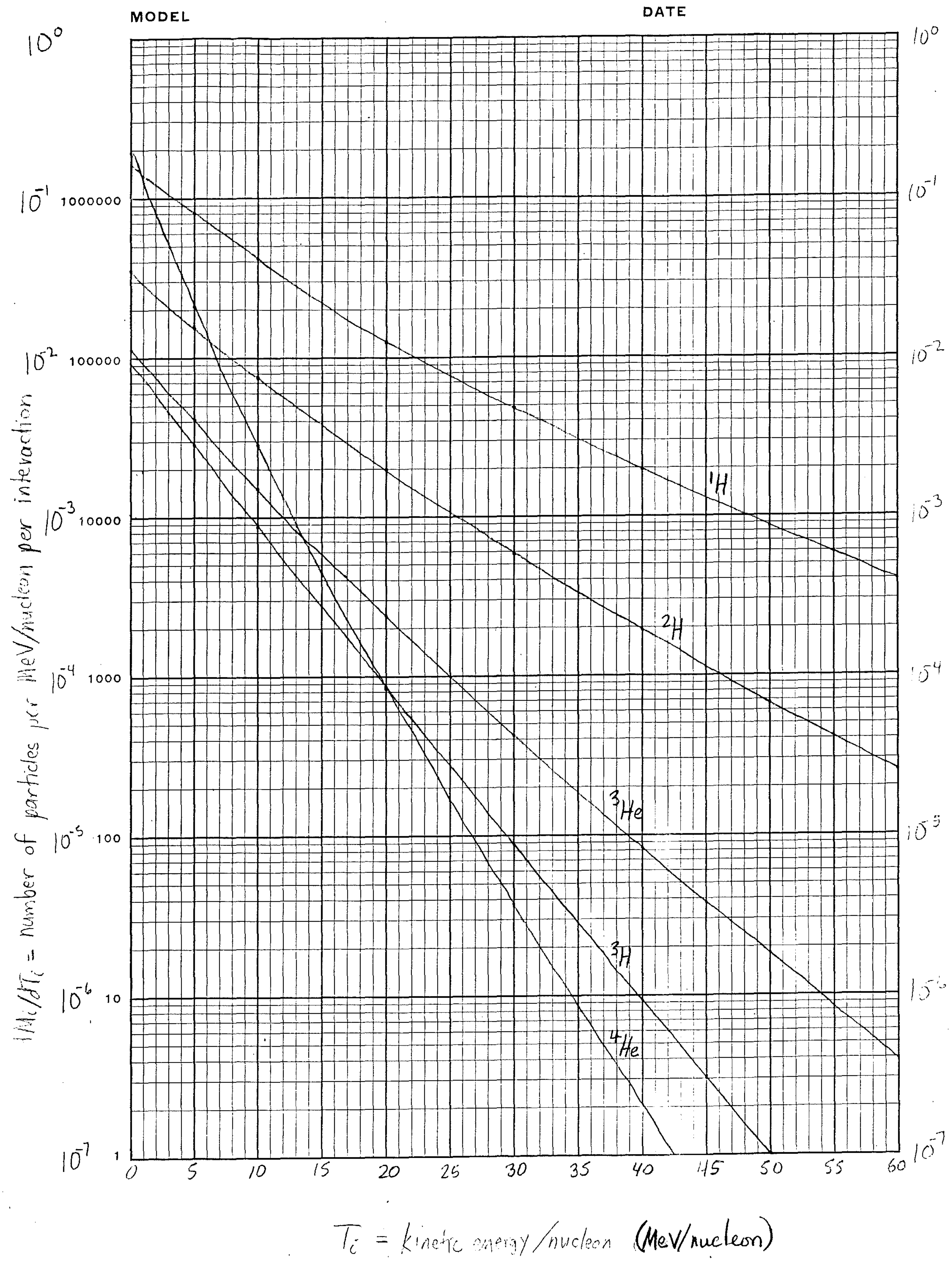

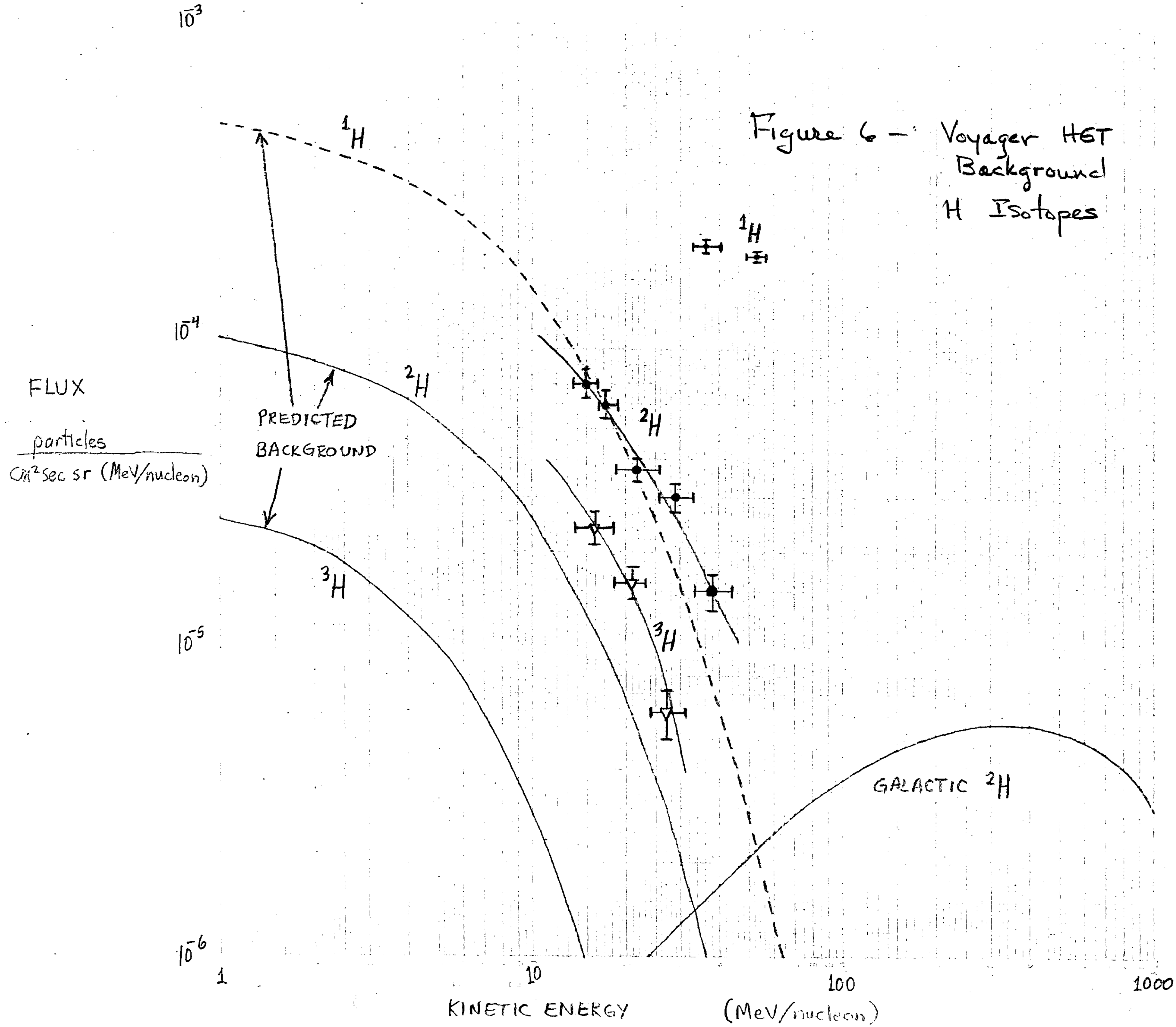

Figure 6 — Voyager HET Background
H Isotopes
10^{-3}
10^{-4}
10^{-5}
10^{-6}
FLUX
particles / cm² sec sr (MeV/nucleon)
PREDICTED BACKGROUND
^1H
^2H
^3H
GALACTIC ^2H
1
10
100
1000
KINETIC ENERGY (MeV/nucleon)

Figure 5 — IMP Measurements and Background

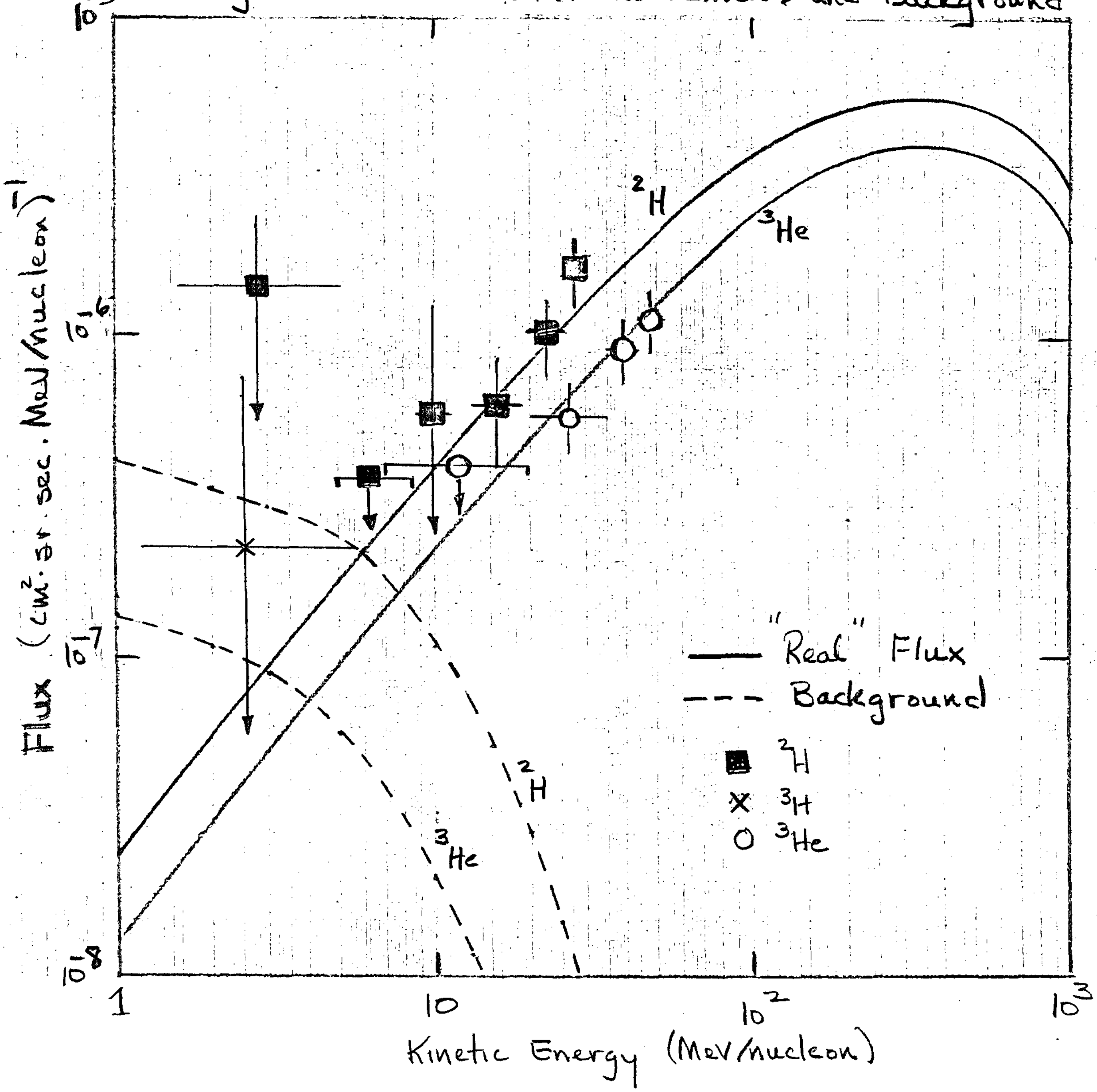

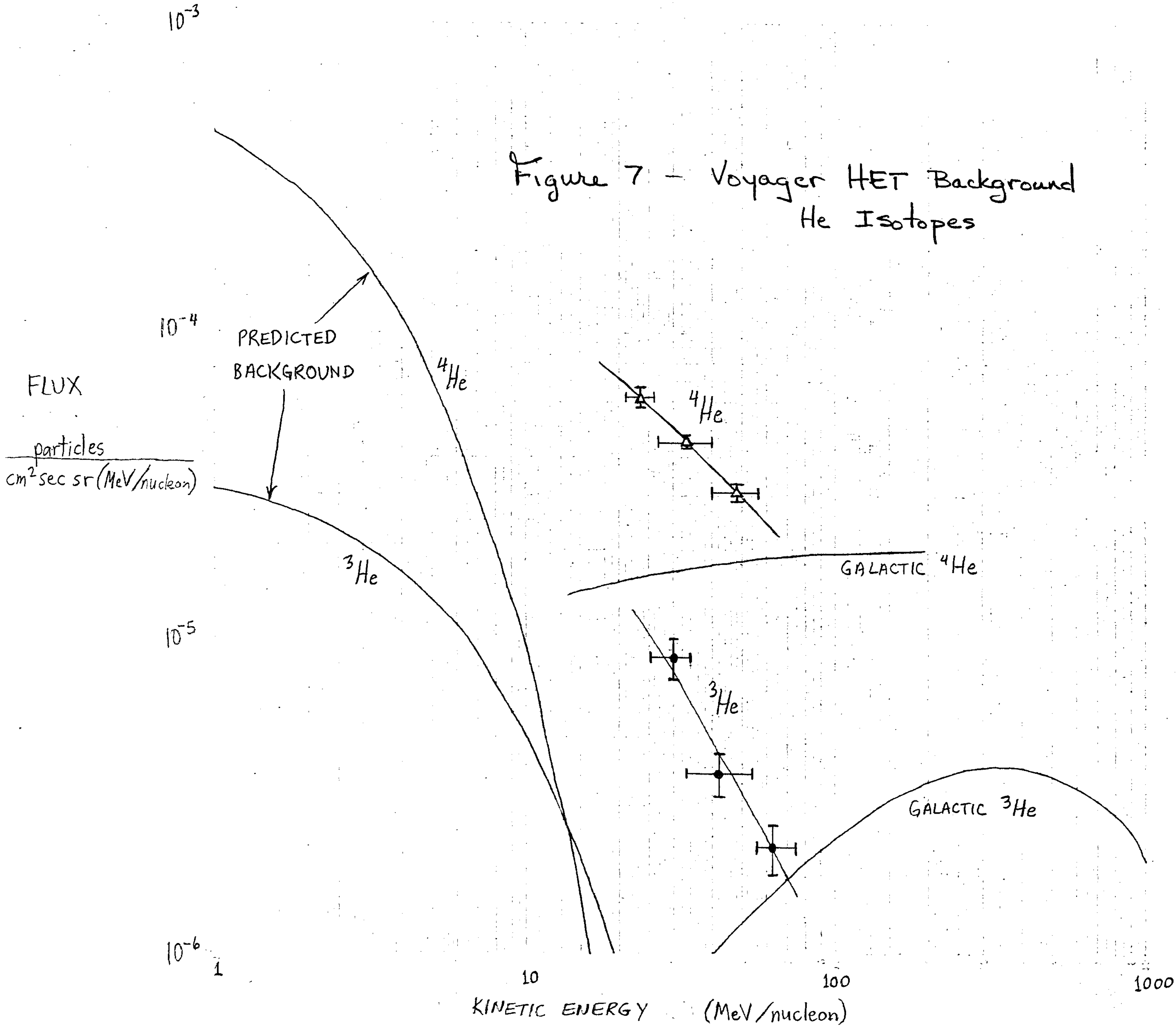

Figure 7 - Voyager HET Background
He Isotopes
10^{-3}
10^{-4}
10^{-5}
10^{-6}
FLUX
particles / cm^2 sec sr (MeV/nucleon)
PREDICTED BACKGROUND
^4He
^3He
^4He
^3He
GALACTIC ^4He
GALACTIC ^3He
1
10
100
1000
KINETIC ENERGY (MeV/nucleon)